Patterns and scaling properties of surface soil moisture in an agricultural landscape: An ecohydrological modeling study

W. Korres, T.G. Reichenau, K. Schneider *

Hydrogeography and Climatology Research Group, Institute of Geography, University of Cologne, D-50923 Köln, Germany

SUMMARY

Soil moisture is a key variable in hydrology, meteorology and agriculture. Soil moisture, and surface soil moisture in particular, is highly variable in space and time. Its spatial and temporal patterns in agricultural landscapes are affected by multiple natural (precipitation, soil, topography, etc.) and agro-economic (soil management, fertilization, etc.) factors, making it difficult to identify unequivocal cause and effect relationships between soil moisture and its driving variables. The goal of this study is to characterize and analyze the spatial and temporal patterns of surface soil moisture (top 20 cm) in an intensively used agricultural landscape (1100 km^2 northern part of the Rur catchment, Western Germany) and to determine the dominant factors and underlying processes controlling these patterns. A second goal is to analyze the scaling behavior of surface soil moisture patterns in order to investigate how spatial scale affects spatial patterns. To achieve these goals, a dynamically coupled, process-based and spatially distributed ecohydrological model was used to analyze the key processes as well as their interactions and feedbacks. The model was validated for two growing seasons for the three main crops in the investigation area: Winter wheat, sugar beet, and maize. This yielded RMSE values for surface soil moisture between 1.8 and 7.8 vol.% and average RMSE values for all three crops of 0.27 kg m^{-2} for total aboveground biomass and 0.93 for green LAI. Large deviations of measured and modeled soil moisture can be explained by a change of the infiltration properties towards the end of the growing season, especially in maize fields. The validated model was used to generate daily surface soil moisture maps, serving as a basis for an autocorrelation analysis of spatial patterns and scale. Outside of the growing season, surface soil moisture patterns at all spatial scales depend mainly upon soil properties. Within the main growing season, larger scale patterns that are induced by soil properties are superimposed by the small scale land use pattern and the resulting small scale variability of evapotranspiration. However, this influence decreases at larger spatial scales. Most precipitation events cause temporarily higher surface soil moisture autocorrelation lengths at all spatial scales for a short time even beyond the autocorrelation lengths induced by soil properties. The relation of daily spatial variance to the spatial scale of the analysis fits a power law scaling function, with negative values of the scaling exponent, indicating a decrease in spatial variability with increasing spatial resolution. High evapotranspiration rates cause an increase in the small scale soil moisture variability, thus leading to large negative values of the scaling exponent. Utilizing a multiple regression analysis, we found that 53% of the variance of the scaling exponent can be explained by a combination of an independent LAI parameter and the antecedent precipitation.

1. Introduction

Soil moisture is a key variable in hydrology, meteorology and agriculture. Particularly surface soil moisture plays a critical role in partitioning precipitation into infiltration and runoff (Western et al., 1999b) and of solar energy into latent and sensible heat fluxes (Entekhabi and Rodriguez-Iturbe, 1994). Soil moisture, and surface soil moisture in particular, is highly variable in space and time. Many factors control its spatial patterns and temporal dynamics, such as topography, soil properties, aspect, land use, management, vegetation, precipitation, solar radiation and specific contributing area (Famiglietti et al., 1998; Hawley et al., 1983; Hebrard et al., 2006; Korres et al., 2010; Rodriguez-Iturbe et al., 2006; Svetlitchnyi et al., 2003; Western et al., 1998, 1999a). Reynolds (1970) distinguished between static (e.g., soil texture, topography) and dynamic (e.g., precipitation, vegetation) controlling factors. Many of these factors are interrelated and most of these factors vary spatially and/or temporally, making it difficult

* Corresponding author. Tel.: +49 221 470 4331; fax: +49 221 470 5124.
E-mail address: karl.schneider@uni-koeln.de (K. Schneider).

to identify unequivocal cause and effect relationships between soil moisture and its driving variables.

In situ measurements of soil moisture are very time consuming and costly, particularly at larger scales. Therefore, great efforts were undertaken to derive spatially distributed soil moisture maps from remote sensing and/or modeling. Many studies have analyzed the spatial structure of soil moisture and its scaling properties using point measurements (e.g. Famiglietti et al., 1998; Western et al., 1998), remotely sensed images (e.g. Kim and Barros, 2002; Koyama et al., 2010; Rodriguez-Iturbe et al., 1995) and model generated maps (e.g. Manfreda et al., 2007; Peters-Lidard et al., 2001). Controversial findings of the relationship between soil moisture variability and mean soil moisture have been reported. Some studies found an increase of spatial variability with decreasing mean soil moisture (Choi and Jacobs, 2011; Famiglietti et al., 1999; Koyama et al., 2010), others found opposite trends (Famiglietti et al., 1998; Western and Grayson, 1998) or were unable to detect a trend (Hawley et al., 1983). Teuling and Troch (2005) showed that both, soil properties and vegetation dynamics, can act to either create or to destroy spatial variability. Rodriguez-Iturbe et al. (1995) and Manfreda et al. (2007) showed a dependency of soil moisture variability on mean soil moisture, which also varies with the spatial scale of the analysis.

Autocorrelation length is often used to analyze the spatial structure of soil moisture fields. For a small grassland catchment, Western et al. (1998) found shorter autocorrelation lengths on wet days, related to the smaller spatial scale of lateral redistribution, in contrast to longer autocorrelation lengths on dry dates, connected to the larger scale of evapotranspiration as the dominant driver. At the field scale (mainly on wheat fields) in a semi-arid climate, Green and Erskine (2004) found a spatial structure of surface soil moisture, but no clear connection of the autocorrelation length to dry or wet soil moisture conditions. Western et al. (2004) compared autocorrelation lengths of soil moisture and terrain attributes, indicating the important role of topography at one site and the variation of soil properties at other sites. However these studies focused on small catchments, mostly with homogeneous vegetation. Therefore the influence of the interacting factors topography, vegetation, soil and meteorology on soil moisture patterns were not investigated.

The main objective of the current study is to characterize and analyze the spatial and temporal patterns of surface soil moisture in an intensively used agricultural landscape and to determine the dominant factors and underlying processes controlling these patterns. A second goal is to analyze the scaling behavior of soil moisture patterns in order to investigate how spatial scale affects these patterns. This is of particular interest for downscaling purposes in order to prevent systematic biases in modeled water and energy fluxes. To achieve these goals, the dynamically coupled, process-based and spatially distributed ecohydrological modeling system DANUBIA was used to analyze the key processes as well as their interactions and feedbacks leading to spatial and temporal soil moisture patterns. Based on the model results we assess the impact of topography, soil, precipitation and vegetation on these patterns. DANUBIA includes a hydrological process model, a plant growth model and a nitrogen turnover model to generate a time series of soil moisture maps for agricultural areas. These maps were subsequently used to derive autocorrelation properties and scaling behavior.

2. Materials and methods

2.1. The DANUBIA simulation system

The DANUBIA simulation system is a component and raster-based modeling tool designed for coupling models of different complexity and temporal resolution. The model framework controls the temporal course of the simulation as well as the dynamic exchange of data at runtime, thus enabling numerous dynamic feedback effects of the various model components. In its complete structure, DANUBIA consists of 17 components, representing natural as well as socio-economic processes (Barth et al., 2004; Barthel et al., 2012). For the current study, only the ecohydrological components regarding plant growth, soil nitrogen transformation, hydrology, and energy balance were used. These components simulate fluxes of water, nitrogen and carbon in the soil–vegetation–atmosphere system using physically-based process descriptions. The relevant processes are computed at hourly or daily time steps. Further information on the open source DANUBIA simulation system is available at www.glowa-danube.de.

A complete description of the model is beyond the scope of this paper and we refer to previous publications of the components involved, namely Mauser and Bach (2009), Klar et al. (2008), Lenz-Wiedemann et al. (2010) and Muerth and Mauser (2012). Thus, we limit our model description here to the fundamental background needed to understand the model setup.

2.1.1. Hydrology and energy balance component

Vertical water fluxes are modeled using a modified Eagleson approach (Eagleson, 1978). The modification particularly pertains to describing water fluxes in soil by a user defined number of soil layers. Percolation of the upper soil layer is interpreted as effective precipitation for the downward layer. Here we used four soil layers (0–5, 5–20, 20–60, 60–200 cm). The uppermost layer is needed to properly model the water available for evaporation from the soil surface. For other processes (e.g., transpiration, plant water uptake, nitrogen turnover and transfer) only three layers are distinguished. Thus, an aggregated top layer is used for these processes by calculating the weighted mean soil moisture of the 0–5 and the 5–20 cm layer.

Volumetric soil moisture and matrix potential is calculated according to the one-dimensional, concentration dependent diffusivity equation (Philip, 1960). Eagleson (1978) presented an analytical solution of the Philips equation for simplified boundary conditions to model the key processes of soil water movement, namely infiltration, exfiltration, percolation and capillary rise. Each layer is assumed to have homogeneous soil characteristics, described by a set of parameters (e.g., thickness, soil texture, bulk density, organic matter content). Based on these soil parameters, hydraulic parameters are calculated using pedo-transfer functions (Brooks and Corey, 1966; Rawls and Brakensiek, 1985; Wösten et al., 1999). Evaporation from interception storage and from the uppermost soil layer is described by a Penman–Monteith approach. For further details, see Mauser and Bach (2009) and Klar et al. (2008).

2.1.2. Plant growth component

The crop growth model simulates water, carbon, and nitrogen fluxes within the crops as well as the energy balance at leaf level. It models photosynthesis, respiration, soil layer-specific water and nitrogen uptake, dynamic allocation of carbon and nitrogen to four plant organs (root, stem, leaf, harvest organ), as well as phenological development and senescence. Resulting from the interplay of these processes, transpiration is a function of available energy, stomatal conductance (controlled by soil moisture and CO_2), and leaf area (emerging from carbon and nitrogen dynamics). The main concepts and algorithms are adopted from the models GECROS (Yin and van Laar, 2005) and CERES (Jones and Kiniry, 1986) with extensions from Streck et al. (2003a,b) for modeling phenological development. For further details, see Lenz-Wiedemann et al. (2010).

2.1.3. Soil nitrogen component

The soil nitrogen transformation model (Klar et al., 2008) is based on algorithms from the CERES maize model (Jones and Kiniry, 1986). The modeled nitrogen transformation processes are mineralization from two organic carbon pools (easily decomposable fresh organic matter and stable humus pool), immobilization, nitrification, denitrification, urea hydrolysis, and nitrate leaching.

2.2. Model validation

Prior to using the model for the analysis of surface soil moisture patterns, the model was thoroughly validated. The model was parameterized using field measurements (e.g., soil texture), data from maps or literature. A site specific calibration of the model was not performed.

2.2.1. Test site and field data

Field measurements for model validation were carried out at the Selhausen test site (50°52′10″N/6°27′4″E, Fig. 1) located in the Rur catchment (Western Germany, see Section 2.3.1) for winter wheat, sugar beet, and maize in the growing seasons 2007/2008 and 2008/2009. A meteorological measurement station and all test fields are located within a 500 m radius of each other.

Continuous soil moisture measurements were taken in 10 cm depth at two different locations at each of the three test fields with FDR soil moisture stations (Delta-T Devices Ltd., Cambridge, UK). The two measurement locations on each field were 5 m apart. The absolute accuracy of measurements is ±3 vol.% with a relative accuracy of ±1% (manufacturer specification, for probe calibration information see Korres et al. (2010). Layer specific soil properties (soil texture, bulk density) for three soil layers (0–30, 30–60, 60–90 cm) were measured according to the sieve–pipette method after DIN 19683-2, 1997 at 20 locations on the winter wheat field in 2007. The measured soil is classified as silt loam with 12% clay, 71% silt and 17% sand for the upper soil layer (mean values from these 20 measurements). The second layer yielded the following clay, silt and sand fractions: 17%, 68%, 15% and the lower soil layer 19%, 66%, 15%. According to the digital soil map provided by the Geological Survey of North Rhine-Westphalia (scaled 1:50,000), all measurement fields have the same soil texture. Thus, the measured mean values were used for all model validation runs with the exception of the maize 2008 field, since the outcrop of an old river terrace of the river Rhine leads to a high amount of gravel on this particular field. Therefore on this field, the layer specific coarse material content was estimated to be 35, 15, and 10 vol.%, respectively.

Soil organic carbon and nitrogen (ammonium and nitrate) content was measured in the same depths at the start of each growing season on all fields to provide field specific initial values for the model. Organic carbon and total nitrogen content were determined with an elemental analyzer (CNS Elemetaranalysator Vario EL, Elementar Analysesysteme GmbH, Hanau, Germany), ammonium and nitrate with a reflectometer (RQflex plus Reflektrometer, Merk, Darmstadt, Germany).

Organ specific fresh and dry biomass and nitrogen content, leaf area index (LAI), phenological stage, plant height and plant density were determined biweekly on up to 14 dates throughout the growing season. Organ specific biomass samples for stem, leaf, and the harvested organ were taken at three locations within each field. After drying of an organ-specific representative aliquot for 24 h at a temperature of 105 °C, average dry biomass was determined. LAI was measured using the LI-3000A Area Meter (LI-COR Bioscience, Lincoln, NE, USA).

Hourly meteorological data (global radiation, precipitation, air temperature, wind speed, air pressure and humidity) were measured at an eddy covariance station (Campbell Scientific, Inc., Logan, USA) located within the winter wheat field. Short data gaps were filled with data from the meteorological tower at the Forschungszentrum Jülich (50°54′37″N/6°24′34″E, distance to Selhausen test fields: 5.1 km). Cloud cover data was taken from the weather station Aachen (German National Weather Service, 50°47′58″N/6°1′30″E, distance to Selhausen test fields: 31.1 km). Precipitation measurements were corrected according to Richter (1995). Due to the close proximity of all test fields to the meteorological station in the winter wheat field, these meteorological measurements were used in all validation runs.

2.2.2. Model parameterization and model validation runs

For model validation, the model was run in point mode (no spatial distribution) for each crop and year. Initial conditions and agricultural management were set as indicated in Table 1. Soil moisture at the beginning of the model period is assumed to be at field capacity. The model runs start at the first of October of the previous year to make sure that the modeled soil moisture is independent of the initial conditions. Soil parameters were set as described in Section 2.2.1. The plant growth model was parameterized according to Lenz-Wiedemann et al. (2010) except for parameters from the phenology model, which were adjusted to field observations of the first year (Table 1).

Modeled surface soil moisture, biomass, and LAI were validated against field measurements using three evaluation criteria, the Root Mean Squared Error (RMSE), the Mean Absolute Error (MAE) and the normalized measure "index of agreement" (Willmott, 1981). The IA is calculated as:

$$IA = 1 - \frac{\sum_{n=1}^{n}(M_i - O_i)^2}{\sum_{i=1}^{n}[|M_i - \bar{O}| + |O_i - \bar{O}|]} \tag{1}$$

where M_i and O_i are simulated and observed values, respectively. $\bar{O}$ is the mean of the observed values and n is the number of data points. A perfect fit between modeled and observed values would result in an IA value of 1.

2.3. Patterns of surface soil moisture

2.3.1. The Rur catchment

The catchment of the river Rur is located in the western part of Germany, covering a total area of 2364 km² with about 140 km² belonging to Belgium and 100 km² to the Netherlands (Fig. 1). The catchment is divided into two major landscape units. The southern part is a low mountain range with forest and grassland characterized by a rolling topography, a mean elevation of about 510 m above sea level, slopes up to 10° and a mean annual precipitation of about 1200 mm.

Our study focuses on the northern part of the Rur catchment (1100 km²), since 46% of the area is farmland. The area is located in the Belgium–Germany loess belt, where crops are grown on a virtually flat terrain (slopes less than 4°). The main crops are winter cereals (mainly winter wheat), sugar beet and maize. The fertile loess plain has a mean elevation of about 100 m above sea level and a mean annual precipitation of about 700 mm. The major soils are Haplic Luvisols and Cumulic Anthrosols near the drainage lines, both with silt loam textures. Soils with a loamy sand texture (Fimic Anthrosols and Dystric Cambisols) are located on the northern edge of the loess plain. Soils close to the Rur are Gleysols and Fluvisols with silty loam and loamy sand textures. Thus, this investigation area is particularly suitable to analyze the effects of vegetation and land use dynamics as well as agricultural management upon soil moisture patterns.
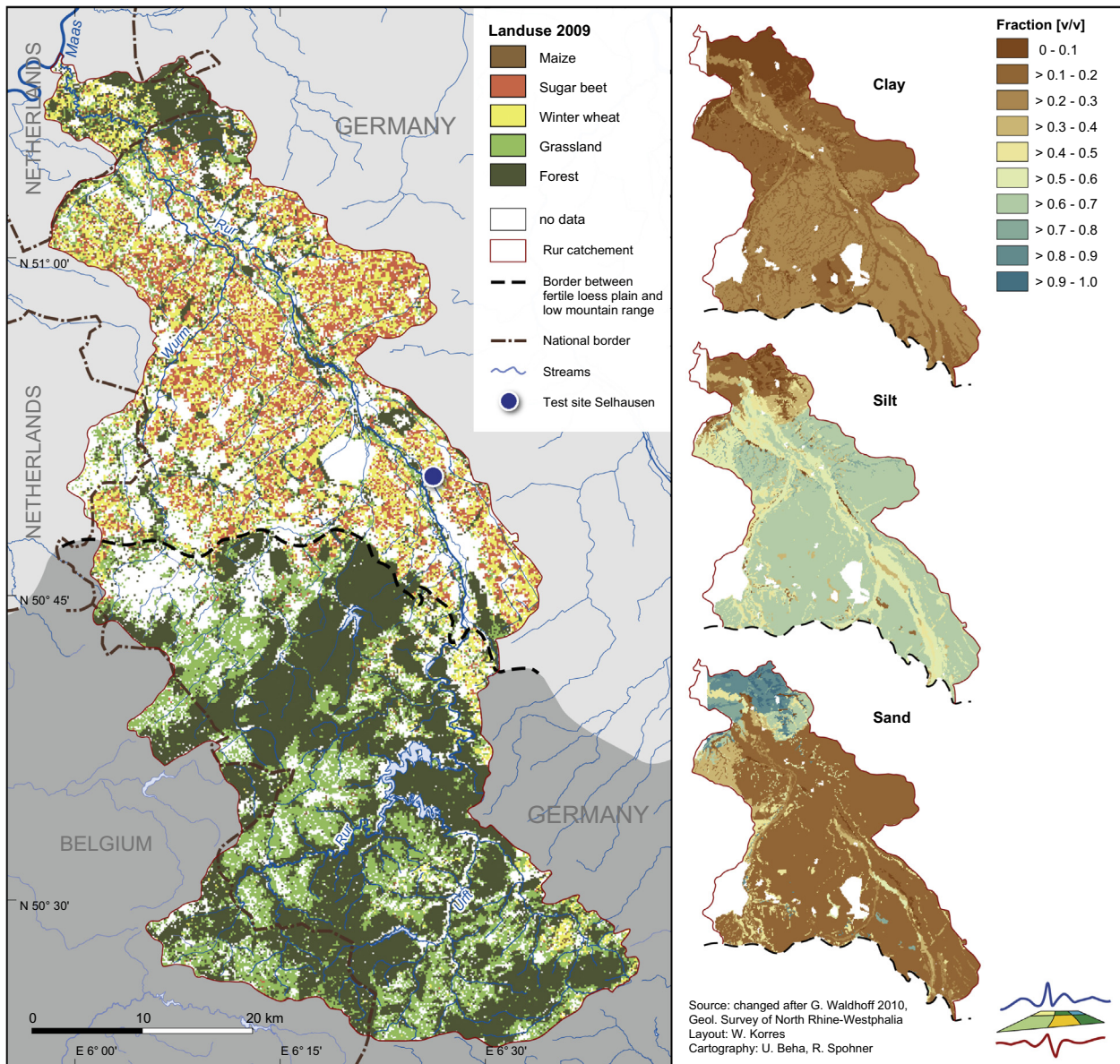
Fig. 1. The Rur catchment with the land use map of 2009, separated into the fertile loess plain in the north and the low mountain range in the south. On the right side, soil texture maps of the top 20 cm of the soil are depicted.

2.3.2. Distributed model runs for northern part of the Rur catchment

Spatially distributed model runs for the year 2009 with a spatial resolution of 150 m were carried out to produce surface soil moisture data for the pattern analysis. Soil properties were derived from a digital soil map (scaled 1:50,000, Geological Survey of North Rhine-Westphalia) for each pixel and soil layer. Land use information (Fig. 1) was gathered from a multitemporal land use classification (Waldhoff, 2010). In the investigation area, 20,299 pixels are classified as cropland (54% winter cereals (parameterized as winter wheat), 41% sugar beet, 5% maize). For spatially distributed model runs, meteorological data from 19 stations of the German National Weather Service within or in direct proximity (<20 km) to the Rur catchment were used to derive the necessary meteorological model input. The measurements were spatially interpolated using the method described by Mauser and Bach (2009). Prior to interpolation, precipitation data was corrected according to Richter (1995). Data on agricultural cultivation as recorded at the Selhausen test site for 2009 (Table 1) was applied throughout the

investigation area. To analyze the respective impact of the spatial patterns of meteorological parameters, land use, and soil properties upon the surface soil moisture patterns, additional model runs were performed using homogeneous inputs for (i) meteorology, using measurements at Selhausen for the whole investigation area, (ii) land use, assuming all agricultural pixels to be winter wheat and (iii) soil texture, using the soil texture of the validation model runs throughout the investigation area.

2.3.3. Pattern analysis

Modeled patterns of daily surface soil moisture on arable land were analyzed in terms of structure, scaling properties and their temporal variation.

2.3.3.1. Structure analysis.
For the analysis of the structure of surface soil moisture patterns, a global spatial autocorrelation coefficient (SAC) was calculated for different step widths. At a step width of 1, each pixel is paired with its direct neighbors in four

Table 1
Initial biomass after sowing, management dates and parameters of the phenology model (R_{max}: maximum daily phenological development rate, V1 denotes the phase from emergence till spikelet initiation, V2 the subsequent phase until start of seed fill, R the seed fill period, see Lenz-Wiedemann et al. (2010)).

Crop and year (of harvest)	Initial biomass (g m^{-2})	Sowing/harvesting date (DOY)	Fertilizer date (DOY)	Feritilizer amount (kg N ha^{-1})		R_{max}, V1 (d^{-1})	R_{max}, V2 (d^{-1})	R_{max}, R (d^{-1})
				Mineral	Organic			
Sugar beet 2008	14.25	114/265	115	80		0.033	0.033	0.012
			135	80				
Sugar beet 2009	14.25	98/288	99	100		0.033	0.033	0.012
			122	60				
Winter wheat 2008	11.875	323/219	59	80		0.026	0.035	0.021
			109	36				
			141		80			
Winter wheat 2009	11.875	291/209	77	60		0.026	0.035	0.021
			104	36				
			139	70				
Maize 2008	4.225	123/277	124	170		0.039	0.039	0.034
Maize 2009	4.225	126/262	127	175		0.039	0.039	0.034
			251		20			

directions (Fig. 2). Pairs with no data values (e.g., due to a non-agricultural land use class) were discarded. The SAC was then calculated as the Pearson correlation coefficient over values of all remaining pairs. For larger step widths, only pairs in the directions of the rook's move in chess were used (Fig. 2). Values of SAC were only calculated for sets of pairs containing a minimum of 100 data pairs, which was the case for all evaluated step widths up to 260. In addition to the analysis of daily soil moisture patterns, the SAC was calculated for spatially distributed soil properties (soil texture).

2.3.3.2. Scaling analysis. Starting from the model's spatial resolution of 150 m, which is referred to as grain size 1, the scaling behavior of surface soil moisture patterns was analyzed by aggregating the pixels to an increasingly coarser grain size of 2 (2×2 pixels), 3 (3×3 pixels), and so forth up to grain size 37 (corresponding to a pixel size of 0.3×0.3 km^2 to 5.55×5.55 km^2). According to Qi and Wu (1996), aggregation starts in the upper left corner of the grid. Aggregated pixels were assigned the mean value of the original pixels. Aggregated pixels were discarded if the totaled area of winter wheat, sugar beet, and maize occupied less than 30% of the pixel area.
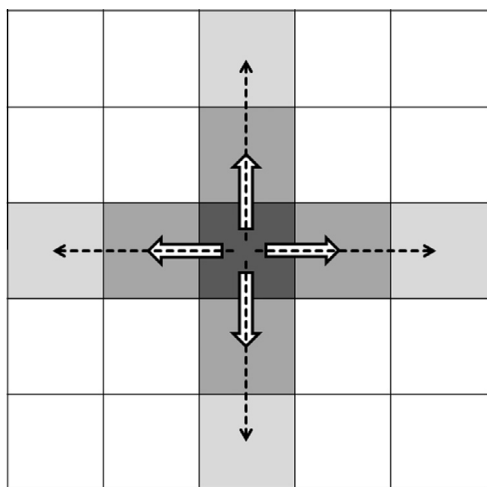

Fig. 2. Exemplary illustration of the pairing for the spatial autocorrelation coefficient for two step widths. For step width 1, the center pixel in dark gray is paired with its four neighbors (bold white arrows). For step width 2, the center pixel is again paired with pixels in four directions, but the distance from the center pixel is extended by one pixel (dashed black arrows). This is done for every pixel and up to a step width of 260.

The scaling behavior of surface soil moisture can be quantified by the slope of a power law relationship computed from the spatial variance (Rodriguez-Iturbe et al., 1995):

$$\sigma_\lambda^2 = \left(\frac{\lambda}{\lambda_0}\right)^\beta \sigma_{\lambda_0}^2 \qquad (2)$$

where λ_0 is the reference scale, λ is the grain size, σ^2 the soil moisture's variance at scale λ, and β is the scaling exponent of the scaling function. β was derived by least square fitting to pairs of λ and σ_λ^2 from grain size 2 to 37, setting λ_0 to grain size 1. A small value of β in absolute value corresponds to a high spatial correlation in the data, a perfect correlation across all computed scales provides a slope value of 0 while no correlation results in a value of -1 (Manfreda et al., 2007; Whittle, 1962).

3. Results and discussion

During the growing season, soil moisture dynamics are strongly influenced by the water uptake of the vegetation. In turn, water demand of the vegetation strongly depends upon vegetation type and development state. Thus it is important, that vegetation dynamics are adequately modeled regarding temporal dynamics as well as spatial patterns. Therefore prior to discussing the results of the model validation for surface soil moisture, we present the validation for the plant growth model.

3.1. Results of the model validation

3.1.1. Biomass and LAI
An overview about the temporal course of key plant parameters (biomass and LAI) for different crops and years is provided in Fig. 3. While the green LAI and the total biomass are of prime importance in the given context, the plant growth model also provides organ specific data for leaf, stem, root and grain. The latter parameters are summarized in Table 2. Fig. 3 shows a very good agreement of the measured and modeled dry matter biomass and LAI. Typically, the model results are within the range of the field measurements denoted by the vertical bars (Fig. 3). Moreover, the model results are very close to observed mean values, despite the large within-field variability especially in the case of the green LAI for sugar beet and winter wheat.

The modeled biomass buildup for winter wheat was slightly delayed in 2008, while the LAI was reproduced quite accurately. In the case of sugar beet, deviations of modeled and measured green LAI are evident from mid-July onwards in both years with a tendency to overestimate in 2008 and underestimate in 2009. Biomass was reproduced very well in 2008. Validation data of dry biomass

for sugar beet in 2009 were not available. The modeled biomass and LAI of maize agrees very well with the measurements.

Table 2 provides an overview about the performance of the plant growth model. For all test fields, the average Root Mean Square Error (RMSE) for the total aboveground biomass is 0.27 kg m^{-2}, which indicates very good agreement between model and measurement. Green LAI is also modeled quite well with an average RMSE of 0.93. Additional measures of model performance are given in Table 2. Moreover the results of the different organs are modeled well, providing evidence that not only the bulk model parameters, but also the processes leading to these results are modeled suitably well.

Leaf area is a limiting factor for transpiration and carbon uptake. Both processes are directly coupled due to common stomatal conductance. The buildup of biomass in turn depends on carbon uptake. Therefore, model performance with respect to green LAI and biomass supports our confidence in the modeled transpiration amounts.

Thus, we are confident that the model performance is sufficiently accurate to adequately simulate key impacts of plant growth dynamics upon the temporal course and spatial dynamics of soil moisture.

3.1.2. Soil moisture: Detailed example

A comparison of modeled and measured soil moisture is presented in Fig. 4 for the example of sugar beet 2008. Since the model was started on the first of October of the previous year, the model results are independent of the assumed initial soil moisture conditions. Due to tillage of the fields, the soil moisture probes were installed in mid-June. Thus no earlier measurements are available. To show the spatial variability of the soil moisture measurements, the measurements of both sampling locations per field are depicted in the figures (Figs. 4 and 5). The statistical indices cited in the text and in Table 3 refer to the average of these two measurements.

The modeled soil moisture in the uppermost layer (Fig. 4) shows distinct peaks related to precipitation events followed by characteristic decreases due to evapotranspiration from the soil surface and percolation into the next soil layer when modeled soil moisture exceeds field capacity (28.6 vol.%). The deeper soil layers show a damped temporal course of the soil moisture. In June, the sugar beet roots reach the lowest soil layer. This is when the modeled soil moisture in the deepest layer starts to decline. A significant recharge of the lowest soil layer was not modeled during the vegetation period. Thus precipitation during the vegetation period is entirely used for evapotranspiration and to a lesser degree for surface runoff.

The model results for the uppermost soil layer agree very well with the measurements at both measurement locations, particularly until mid-July. Thereafter, the model overestimates soil moisture especially immediately after precipitation events but approximates observations in the drying phases. In contrast to the preceding precipitation events where infiltration was only slightly overestimated, in phase II the model simulates an infiltration which is more than twice as high as indicated by measured soil moisture particularly during the precipitation event on 26 July 2008. Starting with that event, modeled soil moisture deviates significantly from observations. During phase I, which we defined as the time prior 16 July 2008, the RMSE is 1.3 vol.%, thereafter (phase II) it increases to 2.0 vol.%, respectively (Table 3). This change in model behavior can be attributed to a change in soil surface properties affecting the infiltration properties. Possible processes leading to the changes at the soil surface might be clogging of the pores by siltation or crust formation. However, these processes might have occurred particularly on loess soils as a result of the strong precipitation event on 10 July 2008 and the following drying period. The model is not calibrated and mod-

el parameters are derived from measured soil texture and pedo-transfer functions. It appears, that at the beginning of the year, this parameterization results in a suitable representation of the infiltration process, while the infiltration process appears to be retarded in the second half of the year. As the soil properties are derived from pedo-transfer functions, a change in surface properties is not represented by the model. To test the assumption of a change of the soil surface conditions, we ran the model for sugar beet 2008 assuming a reduced infiltration capacity of 1.8 mm h^{-1} instead of the original values between 6 and 8 mm h^{-1}. This change resulted in an improvement of the RMSE from 2.0 vol.% to 1.7 vol.% for phase II, while the overall RMSE for the whole period improved from 1.8 vol.% to 1.6 vol.%. A similar effect can be observed for maize 2008 (starting on the same date) and maize 2009 after 6 July 2009. For winter wheat, this effect was not observed (Fig. 5).

3.1.3. Soil moisture: overview

The modeled and measured course of surface soil moisture for all crops for 2008 and 2009 is shown in Fig. 5. For sugar beet 2008 as well as for winter wheat 2008, measured values are reproduced well with RMSE values of 1.8 and 2.1 vol.%, respectively (compare Table 3 and Fig. 5). In the case of winter wheat 2009, RMSE is higher with a value of 2.6 vol.% which is mainly due to overestimation after 27 June 2009. In the case of maize 2008, the model slightly overestimates the measured soil moisture. This may be related to the very high percentage of coarse material in the soil of the maize field 2008 (outcrop of gravel from a former river terrace) causing also relatively low observed surface soil moisture between 6 and 24 vol.% compared to the other validation examples. For both years, the modeled surface soil moisture and the measurements agree well during the first part of the year (phase I). After 16 July 2008 and after 9 July 2009 (beginning of phase II), model results for sugar beet and maize systematically deviate from the measurements: The amplitude of the modeled surface soil moisture is henceforth significantly larger than the observed data. As indicated above in the detailed example of the sugar beet 2008, this behavior hints towards a change in soil surface properties for root crops. Calibrating the infiltration capacity for maize, comparable to sugar beet 2008, RMSE improved during phase II from 7.2 vol.% in 2008 to 3.3 vol.% and from 9.8 vol.% in 2009 to 1.7 vol.% yielding an overall RMSE for the whole period of 3.2 vol.% in 2008 and 2.1 vol.% in 2009. The RMSE between modeled and observed surface soil moisture for both years and all crops ranges from 1.8 to 7.8 vol.% (see Table 3). Considering only phase I for root crops, the RMSE shows values between 1.3 and 3.0 which indicates (a) the good performance of the model and (b) that a change in infiltration conditions occurred for root crop fields and that this effect should be taken into account. As shown above, modeled surface soil moisture has a much lower RMSE at the beginning of the measurements. Therefore, it can be assumed that the RMSE for the whole year is lower than in the validation period. However, an appropriate model to account for the observed change in infiltration conditions is not available.

All results presented above were derived using measured soil parameters from the test site Selhausen. For spatially distributed model runs, a digital soil map provided by the Geological Survey of North Rhine-Westphalia was used. The soil map provides generalized information of the soil texture, thus resulting in a larger uncertainty of the soil parameters as compared to the soil parameterization based on field measurements. Using data from the digital soil map instead of the measured soil data to estimate the model parameters for the test fields in Selhausen yielded an average RMSE of 5.5 vol.% and thus a decrease by 2.1 vol.%. The maize 2008 field was disregarded in this analysis, since it is an
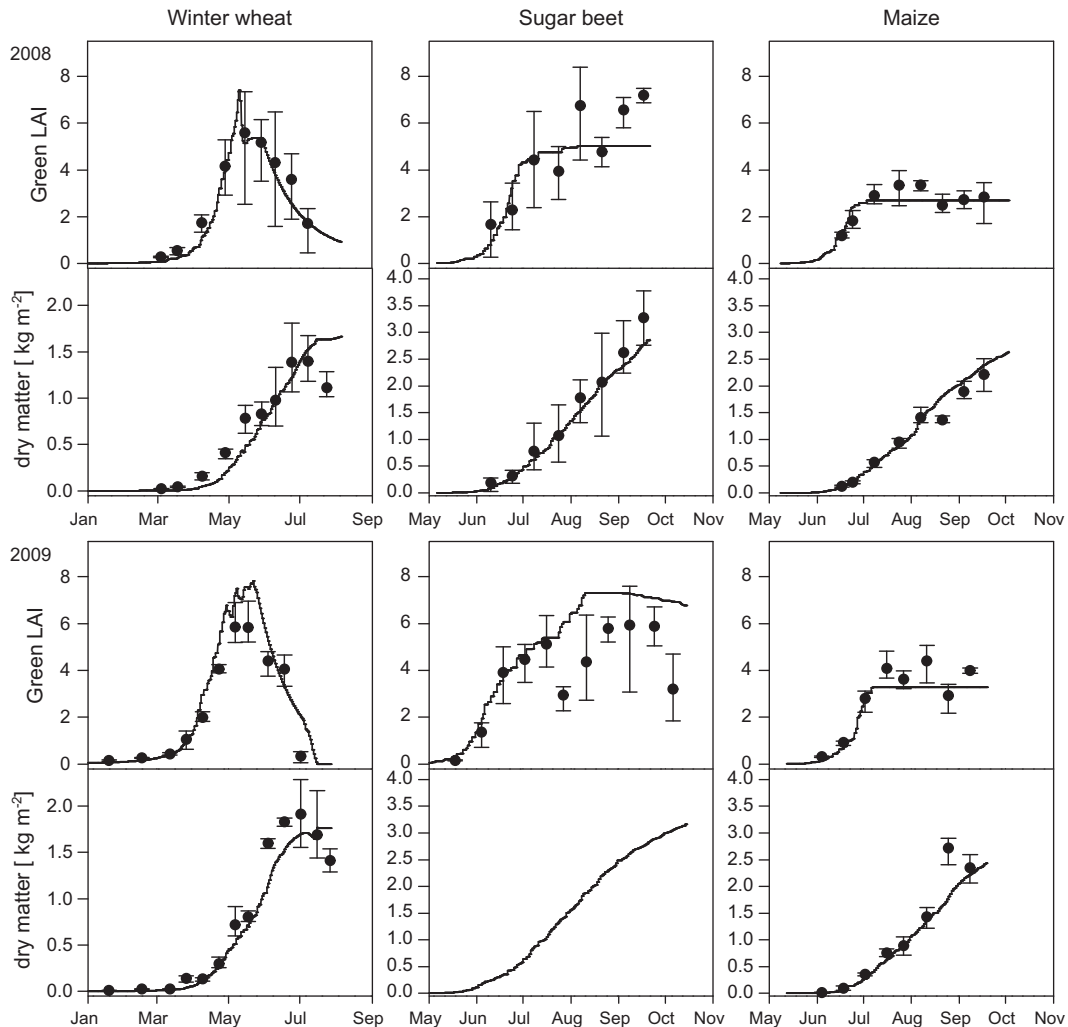
Fig. 3. Green LAI and aboveground biomass (living leaf, stem and harvest organ dry biomass) for winter wheat, sugar beet and maize for the years (of harvest) 2008 and 2009. Measured values (field means) are depicted as dots, bars represent the span of the measurements, and modeled values are displayed as lines. Field measurements of the sugar beet biomass in 2009 were not available.

exceptional case due to its high gravel content and thus is atypical for most of the agricultural area. In general, utilizing the model parameterization based upon the soil map resulted in an overestimation of the soil moisture. This is due to the higher percentage of clay in the soil texture from the soil map, which results in higher field capacities by approx. 5 vol.% as compared to the measured soil texture.

The validation shows that the model simulates plant growth, plant water uptake, and surface soil moisture with sufficient accuracy and thus provides suitable base data for the analysis of surface soil moisture patterns. However, discrepancies between modeled and observed soil moisture, especially in phase II of the growing season, should to be taken into account in further analyses, since these were not corrected in the spatially distributed model runs, since a model to account for these abrupt changes in infiltration properties is currently not available.

3.2. Soil moisture patterns in the Rur catchment

3.2.1. Model results

Fig. 6 shows the temporal course of the spatial mean soil moisture along with the precipitation and evaporation for the investigation area for 2009. The mean surface soil moisture calculated from

the 20,299 pixels is highly responsive to precipitation events. The average spatial mean soil moisture during the main growing season (defined from DOY 103, when LAI of the winter wheat reaches 2, to DOY 288, when sugar beet is harvested) is 26.4 vol.% (Min.: 21.0 vol.%, Max.: 32.6 vol.%). For the rest of the year it is 28.9 vol.% (Min.: 25.0 vol.%, Max.: 33.8 vol.%). The difference in the average soil moisture is mainly due to evapotranspiration. The spatial coefficient of variation (CV, Fig. 6) describes the (mean-) normalized variability of soil moisture and increases during the course of dry periods, while precipitation events lead to a reduction of the CV. Very low CV values are observed in winter and spring until the end of March and in late fall and winter with values around 12%. A period of high CV starts in April with a peak (22%) in the beginning of June, due to the strong spatial variability of water uptake related to the differences in phenological development of winter wheat and sugar beet/maize. After establishment of canopy closure (LAI > 2) by sugar beet and maize, these differences decrease and the CV declines to values of around 14% in mid-July. The second increase of the CV that starts in mid-August and peaks at 23% in the beginning of October is again caused by the different phenological development of wheat and sugar beet/maize. Wheat is harvested earlier (DOY 209), thus the differences in evapotranspiration of bare soil (harvested winter wheat) and the later

Table 2
Results of the model validation for the crop growth model. Indices are the Root Mean Square Error (RMSE), the Mean Absolute Error (MAE), and the Index of Agreement (IA). Aboveground biomass is defined here as the sum of living leaf, stem, and harvest organ dry biomass.

Crop and year (of harvest)	Winter wheat 2008			Winter wheat 2009			Sugar beet 2008			Sugar beet 2009			Maize 2008			Maize 2009		
	RMSE	MAE	IA	RMSE	MAE	IA	RMSE	MAE	IA	RMSE	MAE	IA	RMSE	MAE	IA	RMSE	MAE	IA
Plant variables																		
Green LAI	0.49	0.40	0.98	0.96	0.74	0.96	1.25	1.05	0.84	1.91	1.40	0.81	0.41	0.34	0.85	0.58	0.46	0.95
Living leaf (g m^{-2})	96	85	0.75	41	30	0.96	301	248	0.65	144	109	0.90	70	63	0.63	72	58	0.85
Stem (g m^{-2})	99	84	0.95	239	125	0.90							141	115	0.91	183	106	0.91
Harvest organ (g m^{-2})	101	74	0.99	318	235	0.90	237	198	0.98				117	76	0.99	120	68	0.99
Aboveground biomass (g m^{-2})	278	156	0.96	188	130	0.98	348	217	0.97				194	122	0.98	328	166	0.96

harvested crops (DOY 262 for maize and DOY 288 for sugar beet) together with the low precipitation amounts result in an increase of the CV until the end of September. In general a highly significant negative exponential relationship between the CV and the mean surface soil moisture (msm) can be found (*p*-value: 0.01):

$$CV = 97.495e^{-0.069msm} \quad (R^2 = 0.75) \tag{3}$$

In agreement with findings of other studies (Choi and Jacobs, 2007, 2011; Famiglietti et al., 1999; Koyama et al., 2010) the variability of surface soil moisture patterns increases with decreasing mean soil moisture. Some studies also found positive relationships between mean soil moisture and soil moisture variability. However, these investigations were conducted on hill slopes or at small catchments scale with homogeneous land use (grassland) and with significant slopes (Famiglietti et al., 1998; Western and Grayson, 1998). The combined effects of soil texture, vegetation, topography, and scale of analysis may lead to different relationships between spatial variability and mean soil moisture (Famiglietti et al., 1998).

The average CV over time (CV separately calculated for the whole year time series of every pixel and then averaged over all pixels) is highest for the second layer (layer 1: 11.0%, layer 2: 14.0% and layer 3: 11.4%) due to the replenishing effect of precipitation in the top soil layer and the larger thickness and water storage capacity of the bottom layer. The dependence of the temporal soil moisture upon precipitation events and soil layer depth becomes evident by calculating the temporal CV for a 10 days moving window. The highest short time temporal variability was found for the uppermost soil layer (CV: 5.7%), while layer 2 provides a CV-value of 2.6% and layer 3 1.0%.

The spatial distribution and variability of the modeled surface soil moisture is shown exemplarily for 2 days: 29 January 2009 (DOY 29) and 21 August 2009 (DOY 233) (Fig. 7). For reasons of comparability, the dates were chosen with the condition that no precipitation occurred in the whole catchment on five consecutive prior days. DOY 29 shows a slightly higher mean value of 27.4 vol.% as compared to 25.6 vol.% on DOY 233. Both maps show very dry areas in the sandy north-western part and very wet areas mostly in proximity to the river Rur. The high values are due to soils with high organic content or high clay content. The general soil moisture patterns are determined by the pattern of the soil texture, particularly on DOY 29 (compare Fig. 1). While large scale soil moisture patterns relating to the soil texture are still discernible in summer, strong small scale variability can also be observed. The large small scale variability in late August is due to small scale land use patterns and the related differences of evapotranspiration, which range from low values of bare soil (harvested winter wheat) to high values for late season other crops (sugar beet, maize). The spatial CV (13.1% for DOY 29, 17.2% for DOY 233) supports this visual impression.

3.2.2. Spatial patterns

The spatiotemporal patterns of surface soil moisture were analyzed using the spatial autocorrelation coefficient (SAC) for each day of 2009 at step widths (compare Fig. 2) ranging from 1 to 260 pixels (from 150 m distance to 39 km). In Fig. 8, SAC is shown as a color coded two-dimensional graph. The temporal change of autocorrelation is easily visible by tracing the same color code along the time axis. The step width at a certain value of SAC is the autocorrelation length. In order to relate the SAC of the surface soil moisture to influencing parameters, the SAC for soil texture, as well as time series of precipitation and evapotranspiration (mean and standard deviation) are presented. To separate the influences of land use, weather, and soil texture on surface soil moisture patterns, we conducted simulations of reduced complexity by respectively keeping one of these variables spatially homogeneous (Fig. 8B–D). The spatial autocorrelation for soil moisture was computed for: (A) the reference run which represents the full complexity of the investigation area, (B) a uniform land use model run, with winter wheat occupying all 20,299 pixels, (C) a uniform meteorology model run using the measured meteorological values at the Selhausen test site throughout the investigation area, and (D) a homogeneous soil model run assuming the soil properties from Selhausen for each pixel in the investigation area.

In general, SAC declines with increasing step width (Fig. 8) but the course of this decline and therefore the autocorrelation length changes throughout the year. For the first and last quarter of the year, where fields are fallow, all simulations – except for the homogeneous soil simulation – show similar autocorrelation lengths, resembling autocorrelation lengths for soil clay content. As an example, at step with 10 on DOY 75 we calculated an SAC value of 0.46 for surface soil moisture comparable to 0.5 for clay content. This indicates the dominating pattern generating role of the soil in the given period. On the other hand, differences between the reduced complexity simulations and the full simulation are noticeable: The homogeneous land use simulation (Fig. 8B) lacks periods of very low SAC values, the homogeneous meteorology simulation (Fig. 8C) lacks distinctive spikes after precipitation events, and the homogeneous soil simulation (Fig. 8D) shows much higher SAC values. These differences are now examined in more detail.

Considerable deviation between the full simulation (Fig. 8A) and the homogeneous land use simulation (Fig. 8B) starts around DOY 100 where SAC drops below 0.8 at a step width of 1. From this time on, significant evapotranspiration of winter wheat becomes noticeable, which in the full simulation increases spatial variability as the sugar beet and maize areas still lie fallow or are just planted. This also shows up in the standard deviation of evapotranspiration that is much smaller in the homogeneous land use simulation (Fig. 8B). As described in the methods section soil physical properties for the model runs are derived by pedo-transfer functions from soil texture maps. This accounts for the landscape scale variability of soil properties. The small scale variability of soil properties is
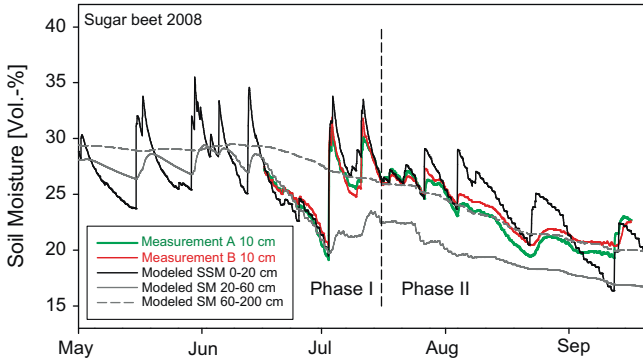
Fig. 4. Modeled and measured surface soil moisture for the sugar beet field 2008.

likely being underestimated in these maps. As a consequence of this simplification in the model runs, the autocorrelation values of the surface soil moisture patterns induced by the soil pattern

might be overestimated. The spatial variability caused by differences in water uptake between the different crops is much larger than that resulting from weather or soil. After harvest of winter wheat on DOY 209, ongoing evapotranspiration of maize and sugar beet contrasted by fallow winter wheat area causes the very low autocorrelation lengths (e.g. SAC value of 0.15 at step width 10 on day 275). These conditions persist until the soil-like patterns re-emerge after all crops are harvested on DOY 288.

In contrast to the full simulation (Fig. 8A), the homogeneous weather simulation (Fig. 8C) does not show the short distinct increases of spatial autocorrelation after precipitation events. During these peaks, autocorrelation lengths rise beyond those for clay content (e.g. SAC value of 0.62 at step width 10 on day 220 compared to an SAC value of 0.5 for clay content). Without the spatial variability of precipitation, the soil is filled at identical rates of precipitation thus preserving or restoring the prevailing patterns induced by the soil. The large scale pattern of precipitation is superimposed on the otherwise prevailing patterns causing increase of correlation lengths (compare Fig. 8A and B). This increase differs between
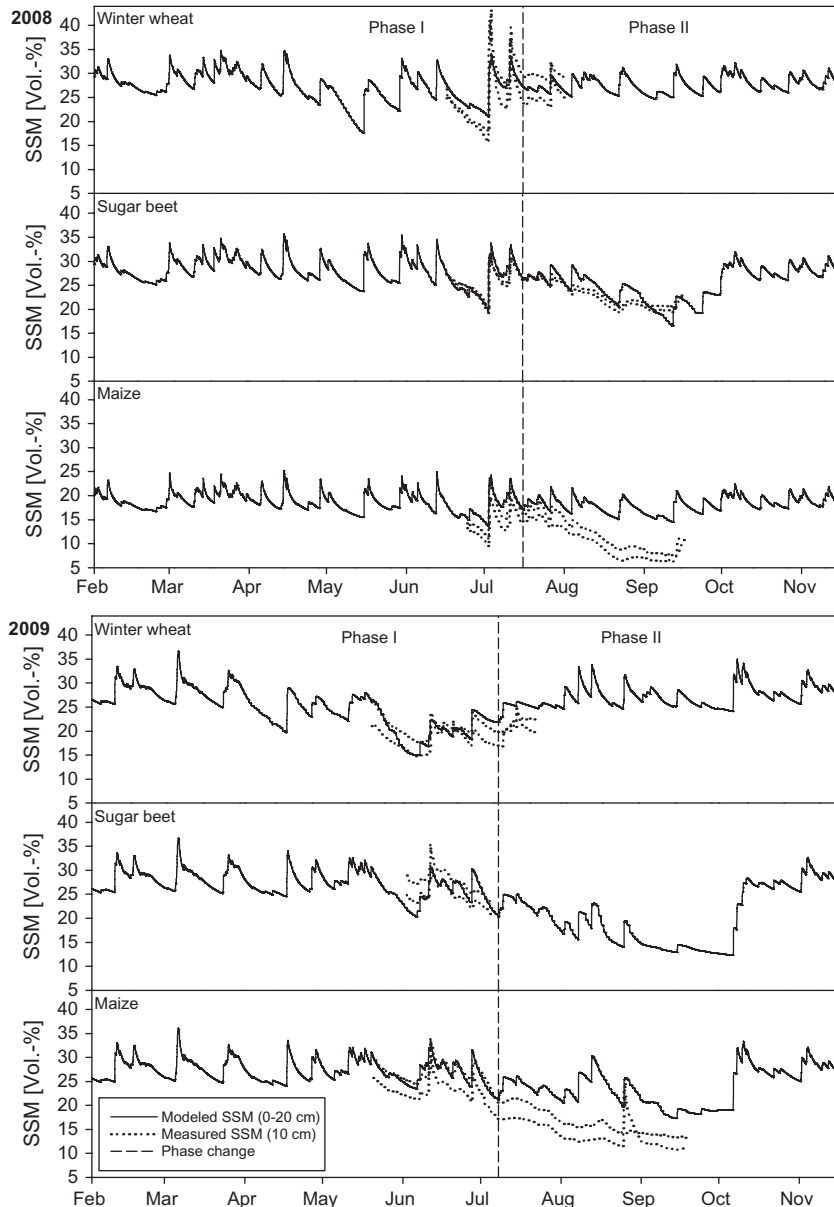

Fig. 5. Modeled and measured surface soil moisture (SSM) for winter wheat, sugar beet and maize for the years (of harvest) 2008 and 2009. The dashed line indicates the change from phase I to phase II.

Table 3

Results of the model validation for surface soil moisture. Indices are the Root Mean Square Error (RMSE), the Mean Absolute Error (MAE), and the Index of Agreement (IA). Phase I + II denotes the indices for the validation over the whole measurement period. The phase change is defined on 16 July (DOY 198) for the year 2008 and 9 July (DOY 190) for the year 2009 and divides the validation period.

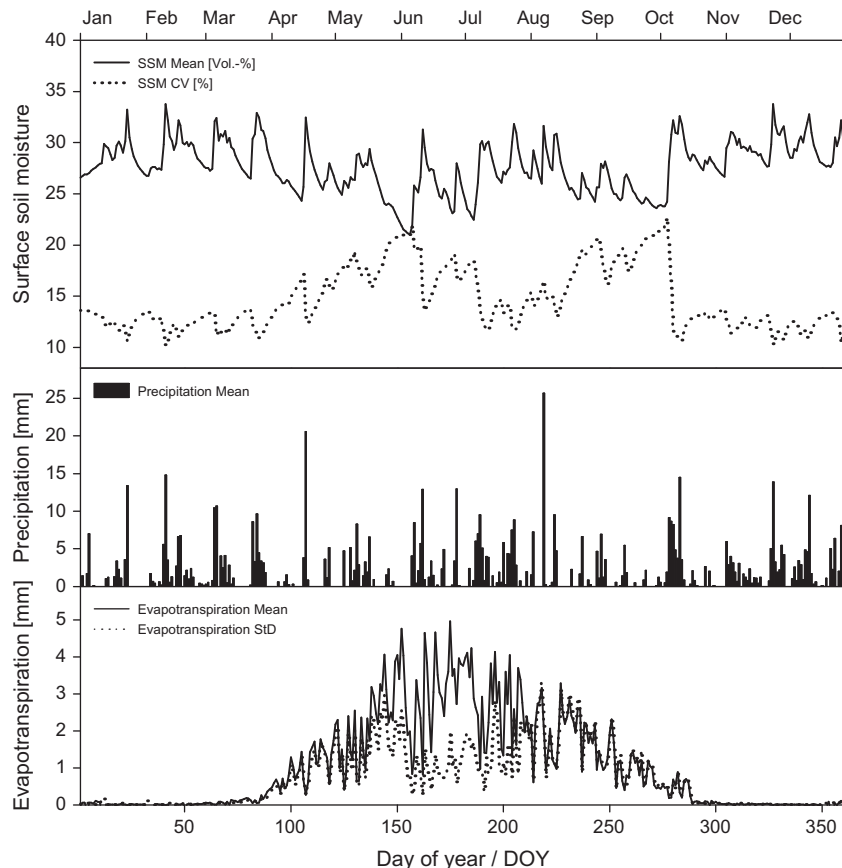| Crop and year (of harvest)	Winter wheat 2008			Winter wheat 2009			Sugar beet 2008			Sugar beet 2009			Maize 2008			Maize 2009		
	RMSE	MAE	IA	RMSE	MAE	IA	RMSE	MAE	IA	RMSE	MAE	IA	RMSE	MAE	IA	RMSE	MAE	IA
Soil moisture (vol.%)																		
Phase I + II	2.1	1.6	0.92	2.6	2.0	0.77	1.8	1.4	0.91				6.4	5.6	0.54	7.8	6.7	0.57
Phase I							1.3	1.0	0.95	2.5	2.0	0.67	3.0	2.8	0.78	2.5	2.3	0.75
Phase II							2.0	1.5	0.87				7.2	6.6	0.47	9.8	9.5	0.31

Fig. 6. Spatial mean surface soil moisture, precipitation and evapotranspiration over all 20,299 pixels of the investigation area of the year 2009. In addition, the coefficient of variation (CV) of surface soil moisture and the standard deviation (StD) of evapotranspiration is depicted with dotted lines.

precipitation events, due to the changing spatial variability and amount of the precipitation and preceding soil moisture conditions. The increase is even more pronounced in the homogeneous land use simulation (Fig. 8B), where the pattern is not disturbed by the small scale spatial variability due to transpiration by different crops.

The high autocorrelation lengths in the homogeneous soil simulation (Fig. 8D) occur outside the main growing season. In that period of time due to the absence of a soil induced pattern and no significant spatial variability of evapotranspiration, soil moisture patterns are predominantly determined by large scale precipitation patterns. Outside the main growing season, in times when no precipitation occurs, soil moisture is characterized by very similar absolute values near field capacity. The absence of precipitation removes all large scale variability induced by the precipitation and thus causing very low autocorrelation lengths (e.g., Fig. 8D at about DOY 30 and 355). During the growing season, the high spatial variability of surface soil moisture due to the het-

erogeneous evapotranspiration persists even during precipitation events preventing high autocorrelation lengths as noticed outside the growing season. Mainly two precipitation events within the growing season result in noticeable autocorrelation lengths. Following these events, starting from overall low soil moisture conditions, the large scale autocorrelation structure of these strong precipitation events is stored in the soil moisture pattern for a longer time period, until it is diminished due to drying caused by evapotranspiration.

Model validation revealed an overestimation of surface soil moisture in the second phase of the growing season for sugar beet and especially for maize. The higher soil moisture makes sugar beet and maize pixels more similar to fallow pixels (winter wheat pixels after harvest). This counteracts the small scale variability of surface soil moisture induced by differences between bare soil and the remaining crops. Without the overestimation, the small scale differences between bare soil and sugar beet or maize were larger, leading to an increased degradation of the larger autocorrelation lengths.
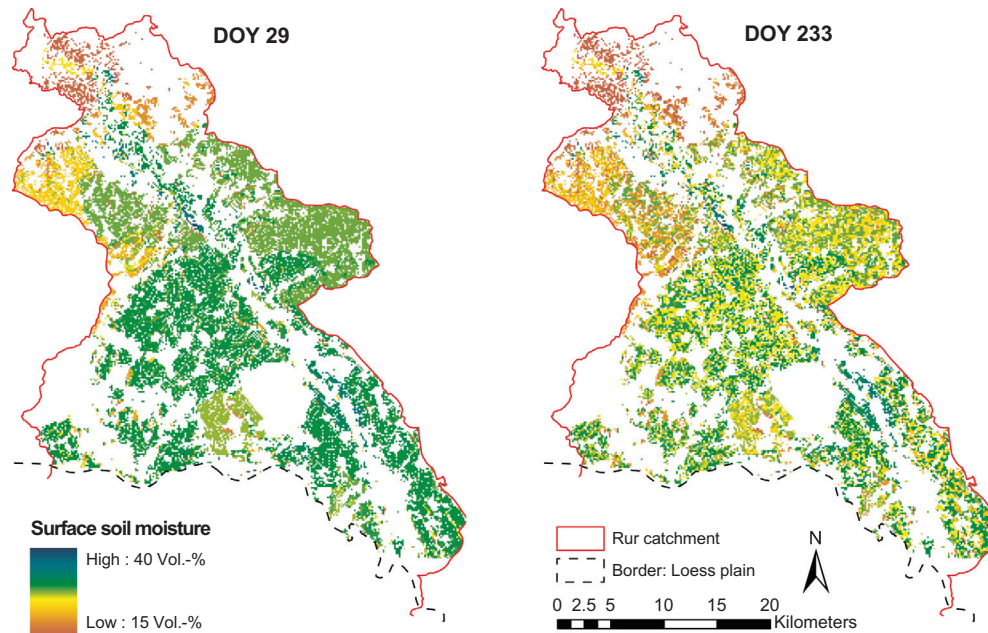
Fig. 7. Spatial distribution of surface soil moisture (top 20 cm) in the investigation area on 29 January (DOY 29) and 21 August 2009 (DOY 233).

In summary, it can be stated that in the beginning of the year at times when the overall soil moisture is high, the surface soil moisture patterns depend upon the soil properties (spatial differences of field capacity). In the main growing season, the larger scale pattern induced by soil properties is diminished by the small scale land use pattern and the resulting small scale variability of evapotranspiration. Due to their high autocorrelation lengths, precipitation events enlarge soil moisture autocorrelation lengths for a short time even beyond the range induced by soil properties. The strength of this effect depends upon the variability and precipitation amount of the events and upon preceding soil moisture conditions. After the growing season, the patterns are again mainly determined by the soil properties.

3.2.3. Scaling

The scaling behavior of patterns is of importance when data are to be scaled down to finer resolutions. Downscaling can be accomplished for instance by relating the global spatial variance of surface soil moisture to the desired scale using a power law relationship (see Section 2.3.3). Fitting the power law function to grain sizes from 2 to 37 for each day of the year resulted in highly significant correlations with R^2 between 0.94 and 0.99. The value of the scaling exponent β varies between −0.17 and −0.62 in the course of the year (Fig. 9) representing the changing scaling behavior of surface soil moisture patterns, which in the analysis above was shown to depend on varying influences of weather, soil, and land use. More negative values of β occur during periods of high small scale spatial variability. Large negative values denote a strong change of surface soil moisture variance with spatial scale, whereas less negative β-values indicate periods of little change of soil moisture variability with spatial scale. The annual course of β closely resembles the autocorrelation lengths found in the pattern analysis stressing a strong relationship between autocorrelation and scaling behavior of spatial variance as described by Whittle (1962). Outside the growing period, β-values found in the current study range from −0.17 to −0.31. This is similar to values found by Rodriguez-Iturbe et al. (1995) and Manfreda et al. (2007). The computed β-values for temporal invariant soil parameters (e.g., −0.23 for clay content, −0.21 for sand content, all with $R^2 > 0.91$) suggest a controlling effect of the soil parameters on the scaling behavior particularly outside of the growing season. However within the growing season, the β-values are well below this range, indicating the strong impact of vegetation dynamics upon the scaling properties of surface soil moisture. As shown above, these low values are caused by the land use pattern and the resulting heterogeneous evapotranspiration particularly towards the end of the growing season. Large precipitation events reset the β-values to values around or even smaller absolute values than −0.25.

To be useable for downscaling, the value of β for a particular day has to be derivable from external variables. A linear equation was fitted to the time series of β and spatial mean surface soil moisture (msm, vol.%) resulting in the following highly significant (p-value: 0.01) relationship:

$$\beta = 0.0158 \text{ msm} - 0.7486 \quad (R^2 = 0.24) \tag{4}$$

The low R^2 value indicates only a weak tendency to less negative values of β at higher mean surface soil moisture, thus showing a limited usability in practical downscaling approaches. Comparable to our study, Manfreda et al. (2007) detected only weak trends over short time periods between mean surface soil moisture values and β, due to the highly variable influence of precipitation and evapotranspiration. A significant influence of drying and wetting cycles on the β-values as in the study of Manfreda et al. (2007) could not be detected.

In order to better understand the main factors determining and predicting the scaling exponent β we analyzed its dependency upon different independent variables. We found that both, the area averaged precipitation cumulated over the previous 20 days (sumPrecip, in mm) and a parameter which expresses the spatial variability of the LAI (devLAI), yield significant correlations to the β-value. To calculate devLAI, we used the results of the validation model run from our test fields for the different crops. From this data a mean LAI of the investigation area was calculated as area weighted average over the different crops. The area weights are taken from the land use classification. devLAI was calculated as an area weighted average of the deviation of the individual crop's LAI from the mean. This procedure makes sure, that devLAI can be
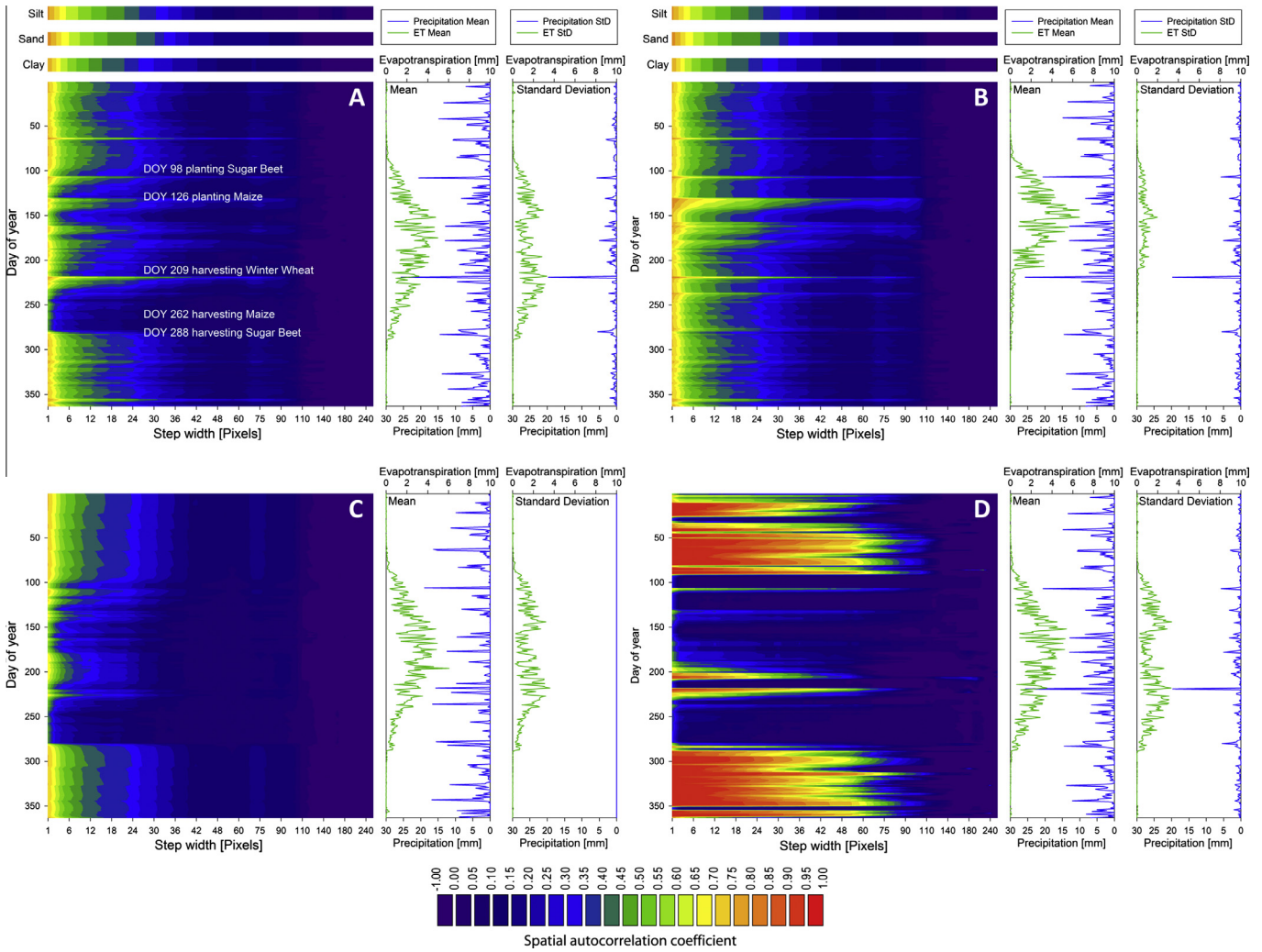
Fig. 8. Spatial autocorrelation coefficient (SAC) of surface soil moisture for different step widths for four different model runs: (A) the reference run which represents the full complexity of the investigation area, (B) a homogeneous land use model run, with winter wheat occupying all 20,299 pixels, (C) a uniform meteorology model run using the measured meteorological values at Selhausen throughout the investigation area, and (D) a homogeneous soil model run assuming the soil properties from the Selhausen test site for each pixel in the investigation area. The temporally constant SAC of soil parameters (fraction of silt, sand, and clay; the same for all model runs) is depicted above and the course of precipitation and evapotranspiration (spatial mean and standard deviation of the investigation area) to the right of the corresponding model run.

derived scale independently from generally available independent data. A linear regression analysis provided highly significant (p-value: 0.01) relationships between sumPrecip and β ($R^2 = 0.19$) and devLAI and β ($R^2 = 0.38$). These results show that the plant related parameter (devLAI) has more predictive power for the scaling parameter β over the whole year than the mean soil moisture state.

Fig. 9. Scaling exponent β of the scaling function for every DOY in 2009.

This indicates once again the importance of the plant controlled water fluxes to explain the soil moisture patterns. Combining the two parameters yields a highly significant (p-value: 0.01), multiple linear relationship:

$$\beta = 0.02 \text{ sumPrecip} - 0.032 \text{ devLAI} - 0.351 \quad (R^2 = 0.53) \quad (5)$$

Thus 53% of the variance of the scaling exponent β can be attributed to the spatial variability of the LAI and to the antecedent precipitation. A multiple regression analysis using devLAI and msm results in an R^2 value of 0.44.

4. Conclusions

A dynamically coupled, process-based and spatially distributed ecohydrological model was used to analyze the key processes as well as their interactions and feedbacks leading to spatial and temporal soil moisture patterns. Based on the model results the impact of soil, precipitation, and vegetation on these patterns was assessed. Because of the strong influence of vegetation water uptake during the growing season in an agricultural landscape, the plant growth model was validated during two growing seasons for the three main crops in the investigation area: Winter wheat, sugar beet, and maize. The average RMSE for the total aboveground
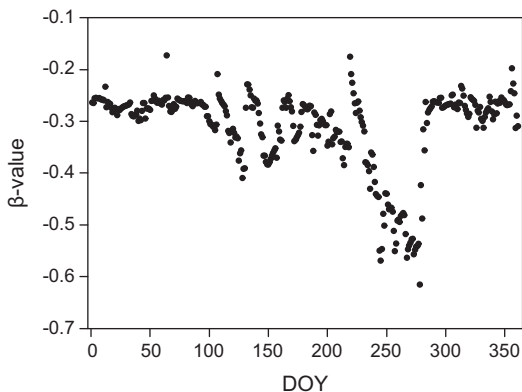
biomass yields a value of 0.27 kg m^{-2}, and 0.93 for green LAI supporting our confidence to adequately simulate the key impacts of plant growth dynamics upon the temporal course and spatial dynamics of soil moisture. The validation of surface soil moisture yields RMSE values that range from 1.8 to 7.8 vol.% for both years and all crops. However, a change in soil infiltration, which was discernible in the field measurements, lead to significantly larger RMSE values for root crops at the end of the growing season. Considering only the first phase of the measurements for root crops, the RMSE shows values between 1.3 and 3.0 vol.%. Possible processes leading to the observed changes in soil infiltration might be clogging of the pores by siltation or crust formation. The validation shows that the model simulates plant growth, plant water uptake, and surface soil moisture with suitable accuracy and thus can provide a suitable base data for the analysis of surface soil moisture patterns and their scaling properties in the northern part of the Rur catchment.

In the northern part of the Rur catchment, the average spatial mean soil moisture during the main growing season is, as expected, lower (26.4 vol.%) as compared to 28.9 vol.% outside the main growing season of 2009. These differences are mainly due to evapotranspiration. A highly significant negative exponential relationship between the coefficient of variation and the mean surface soil moisture was found, meaning that the variability of surface soil moisture increases with decreasing mean soil moisture.

To analyze the patterns of surface soil moisture and their scaling properties, an autocorrelation analysis was conducted. At the beginning and the end of the year when the overall soil moisture is high, surface soil moisture patterns depend mainly on the soil properties (field capacity). During the main growing season, the patterns resulting from soil properties were modified by patterns resulting from the small scale land use pattern and the resulting small scale variability of evapotranspiration. With increasing spatial scales, land use related impacts decrease due to averaging of the small scale evapotranspiration variability. Due to their high autocorrelation lengths, precipitation events increase soil moisture autocorrelation at all spatial scales and even beyond the autocorrelation lengths resulting from the soil properties. The strength of this effect depends on the variability and amount of the precipitation and upon the preceding soil moisture conditions. Scaling properties found in this study depend further on the specific field sizes and management structures in the northern part of the Rur catchment. While the particular scaling properties may not apply to areas with a significantly different agricultural structure, the general finding of field size dominated spatial soil moisture patterns during the main growing period should also apply to other regions. The scale of our investigation was chosen to account for the small scale variability of surface soil moisture caused by heterogeneous land use.

Fitting the daily spatial variance of surface soil moisture to scale for grain sizes between 2 and 37 using a power law relationship yields daily values of the scaling exponent β between -0.17 and -0.62. Large negative values of β occur during periods of high small scale spatial variability and denote a strong decrease of surface soil moisture variability with increasing scale, while less negative β-values indicate periods of reduced scale dependency. Large negative β-values occur mainly during dry periods in summer, which indicate again the influence of small scale variability of evapotranspiration during the growing season. 53% of the variance of the scaling exponent β can be explained by an independent LAI parameter to account for the small scale variability of plant controlled water fluxes and a precipitation parameter to account for the temporal variability of the precipitation. This indicates a potential to assess the subscale surface soil moisture heterogeneity from coarse scale data. Understanding the subscale soil moisture heterogeneity is, for example, particularly relevant to better utilize coarse scale soil moisture data derived from SMOS or future SMAP satellite measurements.

References

Barth, M., Hennicker, R., Kraus, A., Ludwig, M., 2004. DANUBIA: an integrative simulation system for global change research in the Upper Danube Basin. Cybernetics and Systems 35 (7–8), 639–666.

Barthel, R. et al., 2012. Integrated modeling of global change impacts on agriculture and groundwater resources. Water Resources Management 26 (7), 1929–1951.

Brooks, R.H., Corey, A.T., 1966. Properties of porous media affecting fluid flow. Journal of Irrigation and Drainage Division, American Society of, Civil Engineering IR2, 61–88.

Choi, M., Jacobs, J.M., 2007. Soil moisture variability of root zone profiles within SMEX02 remote sensing footprints. Advances in Water Resources 30 (4), 883–896.

Choi, M., Jacobs, J.M., 2011. Spatial soil moisture scaling structure during Soil Moisture Experiment 2005. Hydrological Processes 25 (6), 926–932.

DIN 19683-2, 1997. Bodenuntersuchungsverfahren im Landwirtschaftlichen Wasserbau—Physikalische Laboruntersuchungen, Bestimmung der Korngrößenzusammensetzung nach Vorbehandlung mit Natriumpyrophosphat. Beuth-Verlag GmbH, Berlin.

Eagleson, P.S., 1978. Climate, soil, and vegetation.3. Simplified model of soil-moisture movement in liquid-phase. Water Resources Research 14 (5), 722–730.

Entekhabi, D., Rodriguez-Iturbe, I., 1994. Analytical framework for the characterization of the space–time variability of soil moisture. Advances in Water Resources 17 (1–2), 35–45.

Famiglietti, J.S. et al., 1999. Ground-based investigation of soil moisture variability within remote sensing footprints during the Southern Great Plains 1997 (SGP97) Hydrology Experiment. Water Resources Research 35 (6), 1839–1851.

Famiglietti, J.S., Rudnicki, J.W., Rodell, M., 1998. Variability in surface moisture content along a hillslope transect: Rattlesnake Hill, Texas. Journal of Hydrology 210 (1–4), 259–281.

Green, T.R., Erskine, R.H., 2004. Measurement, scaling, and topographic analyses of spatial crop yield and soil water content. Hydrological Processes 18 (8), 1447–1465.

Hawley, M.E., Jackson, T.J., McCuen, R.H., 1983. Surface soil-moisture variation on small agricultural watersheds. Journal of Hydrology 62 (1–4), 179–200.

Hebrard, O., Voltz, M., Andrieux, P., Moussa, R., 2006. Spatio-temporal distribution of soil surface moisture in a heterogeneously farmed Mediterranean catchment. Journal of Hydrology 329 (1–2), 110–121.

Jones, C.A., Kiniry, J.R., 1986. CERES-Maize: A simulation Model of Maize Growth and Development. Texas A&M University Press, College Station, 194 pp.

Kim, G., Barros, A.P., 2002. Space–time characterization of soil moisture from passive microwave remotely sensed imagery and ancillary data. Remote Sensing of Environment 81 (2–3), 393–403.

Klar, C.W., Fiener, P., Neuhaus, P., Lenz-Wiedemann, V.I.S., Schneider, K., 2008. Modelling of soil nitrogen dynamics within the decision support system DANUBIA. Ecological Modelling 217 (1–2), 181–196.

Korres, W., Koyama, C.N., Fiener, P., Schneider, K., 2010. Analysis of surface soil moisture patterns in agricultural landscapes using Empirical Orthogonal Functions. Hydrology and Earth System Sciences 14 (5), 751–764.

Koyama, C.N., Korres, W., Fiener, P., Schneider, K., 2010. Variability of surface soil moisture observed from multitemporal C-band synthetic aperture radar and field data. Vadose Zone Journal 9 (4), 1014–1024.

Lenz-Wiedemann, V.I.S., Klar, C.W., Schneider, K., 2010. Development and test of a crop growth model for application within a Global Change decision support system. Ecological Modelling 221 (2), 314–329.

Manfreda, S., McCabe, M.F., Fiorentino, M., Rodríguez-Iturbe, I., Wood, E.F., 2007. Scaling characteristics of spatial patterns of soil moisture from distributed modelling. Advances in Water Resources 30 (10), 2145–2150.

Mauser, W., Bach, H., 2009. PROMET – large scale distributed hydrological modelling to study the impact of climate change on the water flows of mountain watersheds. Journal of Hydrology 376 (3–4), 362–377.

Muerth, M., Mauser, W., 2012. Rigorous evaluation of a soil heat transfer model for mesoscale climate change impact studies. Environmental Modelling and Software 35, 149–162.

Peters-Lidard, C.D., Pan, F., Wood, E.F., 2001. A re-examination of modeled and measured soil moisture spatial variability and its implications for land surface modeling. Advances in Water Resources 24 (9–10), 1069–1083.

Philip, J.R., 1960. General method of exact solution of the concentration-dependent diffusion equation. Australian Journal of Physics 13, 1–12.

Qi, Y., Wu, J.G., 1996. Effects of changing spatial resolution on the results of landscape pattern analysis using spatial autocorrelation indices. Landscape Ecol 11 (1), 39–49.

Rawls, W.J., Brakensiek, D.L., 1985. Predictions of Soil Water Properties for Hydrologic Modelling, New York, pp. 293–299.

Reynolds, S.G., 1970. The gravimetric method of soil moisture determination, Part III. An examination of factors influencing soil moisture variability. Journal of Hydrology 11 (3), 288–300.

Richter, D., 1995. Ergebnisse methodischer Untersuchungen zur Korrektur des systematischen Meßfehlers des Hellmann-Niederschlagsmessers. Berichte des Deutschen Wetterdienstes, 194, Offenbach am Rhein, 93 pp.

Rodriguez-Iturbe, I., Isham, V., Cox, D.R., Manfreda, S., Porporato, A., 2006. Space–time modeling of soil moisture: stochastic rainfall forcing with heterogeneous vegetation. Water Resources Research 42 (6), W06D05.

Rodriguez-Iturbe, I. et al., 1995. On the spatial-organization of soil-moisture fields. Geophysical Research Letters 22 (20), 2757–2760.

Streck, N.A., Weiss, A., Baenziger, P.S., 2003a. A generalized vernalization response function for winter wheat. Agronomy Journal 95 (1), 155–159.

Streck, N.A., Weiss, A., Xue, Q., Baenziger, P.S., 2003b. Improving predictions of developmental stages in winter wheat: a modified Wang and Engel model. Agricultural and Forest Meteorology 115 (3–4), 139–150.

Svetlitchnyi, A.A., Plotnitskiy, S.V., Stepovaya, O.Y., 2003. Spatial distribution of soil moisture content within catchments and its modelling on the basis of topographic data. Journal of Hydrology 277 (1–2), 50–60.

Teuling, A.J., Troch, P.A., 2005. Improved understanding of soil moisture variability dynamics. Geophysical Research Letters 32 (5), L05404.

Waldhoff, G., 2010. Land Use Classification of 2009 for the Rur Catchment.

Western, A.W., Blöschl, G., Grayson, R.B., 1998. Geostatistical characterisation of soil moisture patterns in the Tarrawarra a catchment. Journal of Hydrology 205 (1–2), 20–37.

Western, A.W., Grayson, R.B., 1998. The Tarrawarra data set: soil moisture patterns, soil characteristics, and hydrological flux measurements. Water Resources Research 34 (10), 2765–2768.

Western, A.W., Grayson, R.B., Blöschl, G., Willgoose, G.R., McMahon, T.A., 1999a. Observed spatial organization of soil moisture and its relation to terrain indices. Water Resources Research 35 (3), 797–810.

Western, A.W., Grayson, R.B., Green, T.R., 1999b. The Tarrawarra project: high resolution spatial measurement, modelling and analysis of soil moisture and hydrological response. Hydrological Processes 13 (5), 633–652.

Western, A.W. et al., 2004. Spatial correlation of soil moisture in small catchments and its relationship to dominant spatial hydrological processes. Journal of Hydrology 286 (1–4), 113–134.

Whittle, P., 1962. Topographic correlation, power-law covariance functions, and diffusion. Biometrika 49 (3–4), 305–314.

Willmott, C., 1981. On the validation of models. Physical Geography 2, 184–194.

Wösten, J.H.M., Lilly, A., Nemes, A., Le Bas, C., 1999. Development and use of a database of hydraulic properties of European soils. Geoderma 90 (3–4), 169–185.

Yin, X., van Laar, H.H., 2005. Crop Systems Dynamics. Wageningen Academic Publishers, Wageningen, 155 pp.